AUT Journal of Electrical Engineering

AUT J. Elec. Eng., 57(3) (2025) 569-588
DOI: 10.22060/eej.2025.24194.5660

Microgrid Operation Optimization Using Optimal Locating and Sizing of PHEV Parking Lots Considering Various Uncertainties

Mehran Alizadeh, Reza Eslami*, Amirreza Salmani

Faculty of Electrical Engineering, Sahand University of Technology, Tabriz, Iran.

ABSTRACT: Microgrids, as a novel structure in power systems, utilize renewable energy sources and vehicle-to-grid (V2G) technology to enhance efficiency, reduce losses, and improve network reliability. This article investigates the optimal operation of a microgrid through the locating and sizing of parking lots for plug-in hybrid electric vehicles (PHEVs) while considering various uncertainties. The study is conducted in two stages. Initially, a comprehensive model is presented for the locating and sizing of parking lots and distributed generation (DG) resources, aiming to minimize operational costs, power losses, and construction costs in a 69-bus network. In the second stage, the optimal operation of the microgrid is analyzed with objectives such as energy management, optimal control of charging and discharging, increasing user profits, reducing losses, and improving network reliability. Uncertainties such as load forecasting, renewable resource generation, travel patterns, and battery charge levels are modeled using probability distribution functions and scenario generation and reduction methods. For both stages, a hybrid PSO-GA algorithm is employed.

Review History:
Received: May, 25, 2025
Revised: Jul. 31, 2025
Accepted: Aug. 19, 2025
Available Online: Oct. 20, 2025

Keywords:
Optimal Control of Charging and Discharging
Distributed Generation
Operational Costs
Power Losses
Energy Management

1- Introduction

The growing demand for energy, depletion of fossil fuel reserves, and environmental concerns have made the use of distributed generation (DG) resources based on renewable energy sources (RES) and electric vehicles a sustainable solution for reducing pollution. In this context, microgrids (MGs), as a novel structure integrating DG resources and electric vehicles with vehicle-to-grid (V2G) capability, provide opportunities for optimizing energy consumption, reducing losses, and enhancing reliability. With grid connectivity, they offer unique opportunities for optimizing energy consumption and reducing network load, leading to improved system efficiency, reduced losses, and increased reliability, as introduced in [1-3]. Microgrids, capable of operating independently or connected to the grid, enhance stability, reduce losses, and optimize energy distribution during emergencies. Electric vehicles, in addition to reducing environmental pollution, play a significant role in power systems by providing services such as peak load management and frequency regulation. However, uncoordinated charging and unpredictable behavior of these vehicles can lead to increased peak loads, voltage deviations, and energy losses [4]. Nevertheless, implementing strategic programs for optimal and managed charging and discharging strategies can mitigate these effects and improve system security and stability [5]. It is necessary to define locations under the title of electric vehicle parking lots (PLs) within the power network so that operators can manage demand to prevent disruptions in microgrids and, through participation in the energy market, provide various benefits for vehicle owners and the power network. These benefits are realized only if parking lots are optimally located and sized, and precise charging and discharging schedules are implemented [6]. Improper installation or mismanagement of parking lots can lead to increased losses, reduced power quality, decreased reliability, and higher operational costs.

Reference [7] addresses the simultaneous allocation of electric vehicle parking lots and renewable resources in distribution networks. The objective is to reduce power losses, improve network stability, and optimize resources. The model considers investment costs and uncertainties but does not examine the V2G mode. A multi-objective particle swarm optimization (MOPSO) algorithm is used. Reference [8] proposes an optimal method for locating and sizing electric vehicle charging stations using a balanced metaheuristic algorithm. The main goal is to improve voltage profiles, reduce active and reactive power losses, and minimize station development costs and voltage deviations. However, V2G capability and DG penetration are not considered. Reference [9] focuses on determining the optimal location and size of parking lots for plug-in electric vehicles

*Corresponding author's email: eslami@sut.ac.ir

in distribution networks, aiming to reduce power losses, improve voltage profiles, enhance system reliability, and increase revenues. This study considers uncertainties such as charge status, the number of connected PHEVs, and varying battery capacities. Reference [10] addresses the locating of an optimal combination of different types of electric vehicle chargers to effectively manage load, reduce installation costs, losses, and transformer loading. The model incorporates the effects of photovoltaic generation and models EV load as a stochastic process. The results show significant reductions in costs, losses, and transformer congestion. Reference [11] optimizes the location and capacity of electric vehicle parking lots and distributed generation in a microgrid using a two-stage genetic algorithm (GA) and particle swarm optimization (PSO). The goal is to improve energy management while considering technical, economic, and environmental aspects. Uncertainties such as vehicle movement and initial charge are also considered, with simulations performed on a standard 33-bus network, including active and reactive power injection by charging stations to enhance energy management.

Reference [2] proposes an optimal operational approach for a microgrid system that includes wind turbines, solar photovoltaic systems, battery energy storage systems, electric vehicles, and demand response. The objective is to minimize the total operational cost of the microgrid by optimizing the use of these components and demand response. It considers the costs of power exchange between the main grid and the microgrid, as well as the costs of electricity generation from the mentioned components. Reference [12] addresses the optimal scheduling of plug-in electric vehicles and a renewable microgrid in energy and reserve markets. The goal is to reduce costs and increase profits for microgrid and vehicle owners. Using a stochastic framework, uncertainties such as wind speed, price, and demand are modeled. The problem is formulated as a mixed-integer linear programming problem considering operational constraints required by PHEV users, with objectives including minimizing overall microgrid costs, PHEV battery consumption, peak load, scenario fluctuations, and planning costs. Reference [13] discusses the optimal operation of a grid-connected AC microgrid considering demand response, plug-in hybrid electric vehicles, and smart transformers. It proposes algorithms and models to minimize operational costs, reduce system losses, and improve voltage profiles. The study includes stochastic modeling to address uncertainties in renewable energy generation, load demand, PHEV charging, and grid energy prices.

Based on the reviewed studies, it can be concluded that the issue of parking lot locating is generally examined from three different perspectives, sometimes in combination: the perspective of network operators, electric vehicle owners, and charging station owners within a power network. The V2G issue has received less attention. Microgrids, as key players in future networks with distributed generation resources and controllable loads, can operate independently or be connected to the upstream network. While most research has focused on energy management and the impact of plug-in hybrid electric vehicles, the locating of parking lots and V2G capability have been less addressed, and uncertainties related to charging demand, resource generation, and electricity prices are often overlooked. In the continuation of the article, Section 2 explains the main assumptions and the general framework of the problem. Section 3 presents the mathematical model for the optimal locating of parking lots along with the problem constraints. Section 4 analyzes and discusses the results obtained from simulations. Section 5 is dedicated to conclusions.

2- Problem Statement

Based on the conducted research, this article addresses the optimal operation of a microgrid using the locating and sizing of parking lots for plug-in hybrid electric vehicles while considering various uncertainties. This is performed in two stages. In the first stage's objective function, a comprehensive and optimal model is presented for the simultaneous locating and sizing of electric vehicle parking lots and distributed generation resources in a 69-bus microgrid. This is designed to reduce operational costs by minimizing power losses and construction costs of generation resources and parking lots, as shown in the flowchart of Fig. 1.

The simultaneous optimization of DGs and EV parking lots brings several advantages:

- -It enables better coordination between energy production and consumption nodes in the grid.
- -It avoids possible conflicts in local loading conditions, which may arise from the independent siting of DGs and EV charging infrastructure.
- -It leads to a globally optimized configuration that minimizes losses, improves voltage stability, and enhances the overall efficiency of the microgrid.

Furthermore, in the presence of vehicle-to-grid (V2G) functionality, EVs are not only loads but also temporary distributed energy sources, which makes the coordination with DGs even more essential.

In the second stage's objective function, the optimal operation of the microgrid is considered, with objectives including energy management, optimal control of electric vehicle charging and discharging demand considering variable prices, increasing user profits from vehicle-to-grid technology, enhancing reliability, reducing losses, minimizing switching operations, reducing hours of connection to the upstream grid, and maintaining a balance between supply and demand, as shown in the flowchart of Fig. 2. In this section, considering all factors and decision variables, the microgrid's performance is evaluated in both grid-connected and islanded modes. The division into two stages is based on a hierarchical optimization framework, which is commonly used in modern power system planning and operation:

- -The first stage (planning level) deals with long-term decisions, such as optimal siting and sizing of DGs and EV parking lots. These are structural decisions that do not frequently change.
- -The second stage (operational level) focuses on short-term scheduling and control, specifically EV charging/discharging under uncertainty. This includes handling

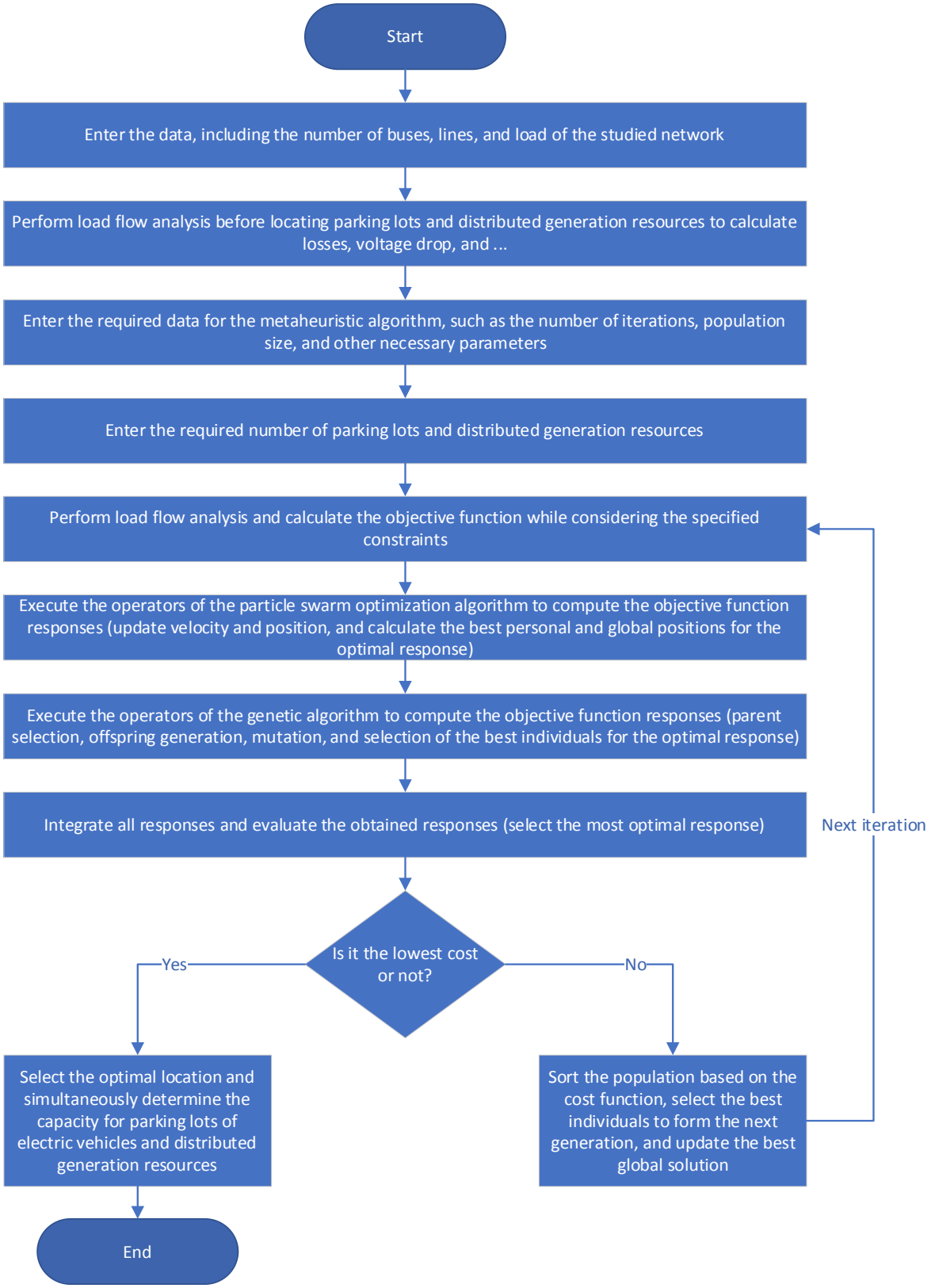

Fig. 1. Flowchart of modeling for implementing the proposed first objective function with the PSO-GA algorithm.

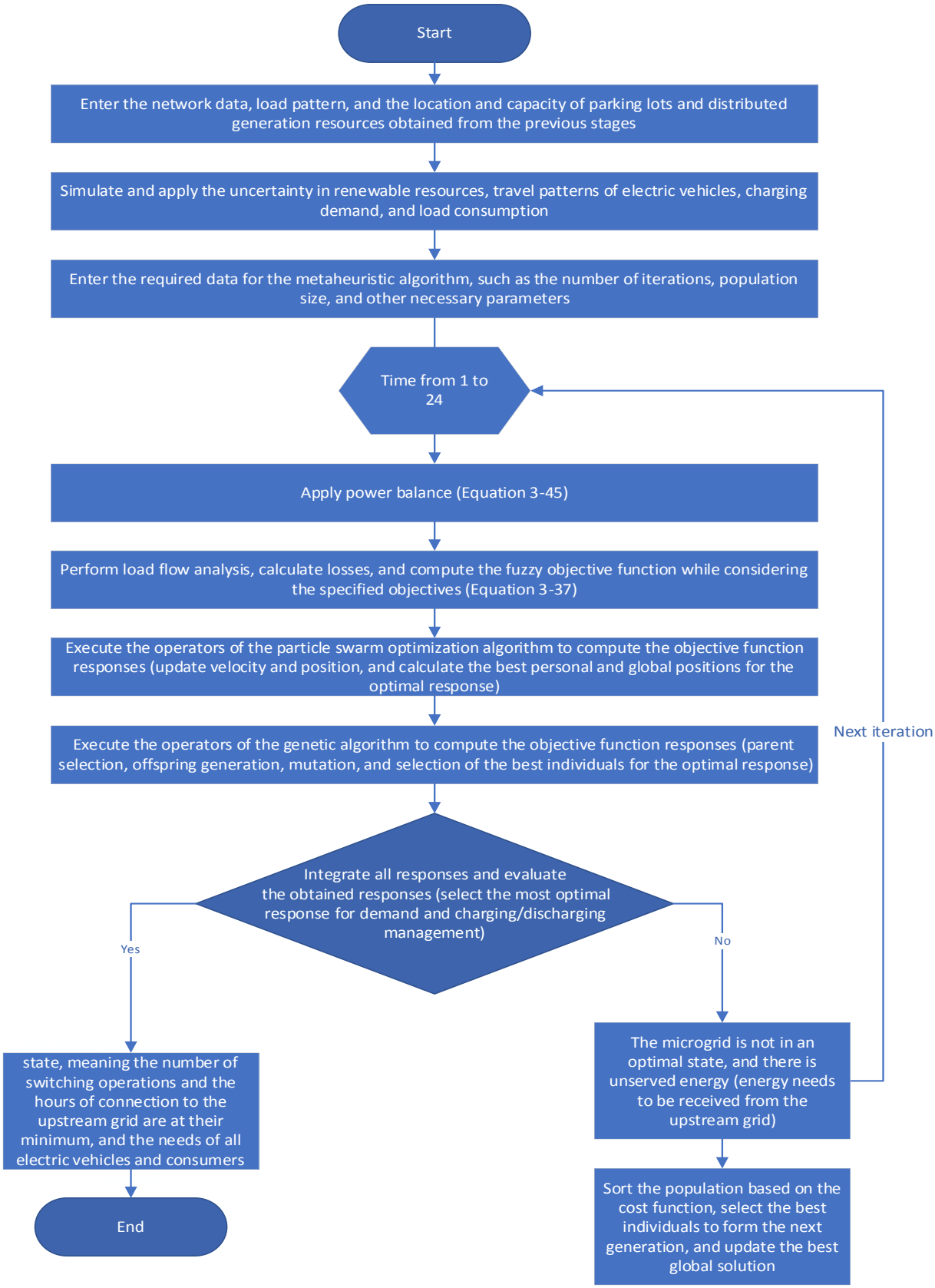

Fig. 2. Flowchart of modeling for implementing the proposed second objective function with the PSO-GA algorithm.

stochastic variables like load profiles, RES generation, EV arrival/departure patterns, and vehicle state of charge (SOC).

Separating these levels allows:

-Decomposition of complex problems into manageable sub-problems

-Reduced computational burden

-Higher solution quality and scalability

Moreover, this separation reflects real-world decision-making hierarchy in smart grid operation, where infrastructure planning and daily operations are handled by different layers of control.

Uncertainties such as load forecasting, renewable resource power generation, travel patterns, vehicle entry and exit times to parking lots, and battery charge levels are considered. To model these uncertainties, various probability distribution functions suitable for each uncertainty are used, along with the scenario generation method. Scenarios that are close to each other are used to accurately simulate the microgrid's operational conditions, providing advanced planning for the charging and discharging of large groups of electric vehicles.

This method not only reduces network costs and limits greenhouse gas emissions due to its reliance on renewable energy but also increases user profits and contributes to system efficiency.

The innovation of this research lies not only in the precise modeling of uncertainties but also in examining the use of electric vehicles as energy storage resources, evaluating their role in the stability and flexibility of the power network. To enhance modeling accuracy, historical data and weather forecasts are used to determine energy generation from renewable resources, and statistical data are used to predict vehicle travel patterns and their charging needs. Another innovation is the proposal of a new approach for power transfer between parking lots and the microgrid using electric vehicles, which, in addition to reducing switching operations, significantly improves the microgrid's reliability. The results demonstrate that the proposed model provides an efficient solution for energy management and reducing operational costs in microgrids. In this thesis, a hybrid PSO-GA algorithm was implemented in both stages of the optimization framework.

The hybrid algorithm was chosen deliberately to benefit from the strengths of both:

-PSO (Particle Swarm Optimization) offers fast convergence and is well-suited for continuous decision variables.

-GA (Genetic Algorithm) provides high exploration capability in complex, non-convex, or discrete problem spaces and helps avoid local minima.

By combining these two, the PSO-GA hybrid algorithm maintains global search ability while also enhancing local convergence. This combination is robust against uncertainties, such as stochastic loads, renewable generation variability, and the random behavior of EVs.

Therefore, the same optimization approach was applied in both planning (DG/PL siting and sizing) and operational (charging/discharging scheduling) stages. The variation lies only in the objective functions and constraints, not in the optimization engine.

The advantage of the proposed method is that it has a definite answer to the problem and does not use an optimal answer obtained from optimization methods.

3- Mathematical Model of the Problem

3- 1- First Objective Function

This section defines a multi-objective function for determining the optimal location and capacity of electric vehicle parking lots and distributed generation resources, incorporating several technical and cost constraints. The primary goal is to reduce construction and loss costs by optimizing the location and capacity of PLs and PHEVs. In this stage, parking lots are modeled solely as loads, calculated according to Eq. (1). The first objective function is a multi-objective model that includes the construction and maintenance costs of distributed generation (DG) resources and parking lots (PLs), active and reactive power losses, and network technical constraints. Using appropriate weighting factors, this function establishes a balance between reducing investment and operational costs, and through the hybrid PSO-GA algorithm, it determines the optimal location and capacity for PLs and DGs.

$$\begin{aligned}\min F(X)_1 &= w_1 \times \mathrm{P}_{Loss} \times C_{Ploss} + w_2 \\ &\times \mathrm{Q}_{\mathrm{Loss}} \times C_{Qloss} + C_{Construction\_DG} \\ &+ C_{Construction\_PL} + C_{Maintenance} + FV\end{aligned} \tag{1}$$

Where w_1 is the Weighting factor for active power losses, w_2 is the Weighting factor for reactive power losses, C_{Ploss} is the Cost of active power losses in the network (per unit of power), and C_{Qloss} is the Cost of reactive power losses in the network (per unit of power).

The weights w_1 and w_2 were determined based on the network's operational priorities and previous researchers' experiences. In this article, the active power loss weight (w_1 = 0.9) was assigned a higher value due to the greater importance of reducing active power losses in operational costs, compared to the reactive power loss weight (w_2 = 0.1). Sensitivity analysis of these weights was conducted in the initial simulation phase, revealing that a ±20% variation in the weights has a minimal impact on optimal locating but significantly affects the relative share of active and reactive power losses in the objective function.

FV: A penalty for non-compliance with network technical specifications (constraints), including an increase in losses exceeding 5%, a voltage drop of 10%, and other restrictions such as not placing PL and DG on the same bus, not placing more than one parking lot or generation resource simultaneously on a bus, and not placing more than two PLs on any network branch. Generally, it is evaluated at the start of the optimization function to ensure that energy generation variables and electric vehicle charging points are within valid ranges without interference. If variables or calculated values

fall outside valid ranges or violate specified conditions, FV increases.

X : The vector of objective function variables, including the location and capacity of electric vehicle charging stations (PL) and the location and capacity of distributed generation resources (DG), obtained using the mentioned metaheuristic algorithm.

$C_{Construction\_DG}$: Total construction cost of distributed generation resources per kilowatt, calculated as:

$$C_{Construction\_DG}=\sum_{i=1}^{r}\left(C_{DG\_i}\times DG_{Capacity\_i}\right) \quad (2)$$

Where C_{DG_i} is the construction cost of the i -th distributed generation resource per kilowatt, $DG_{Capacity\_i}$ represents the capacity of the i -th resource, and r is the number of requested distributed generation resources.

$C_{Construction\_PL}$: Total construction cost of plug-in hybrid electric vehicle parking lots per kilowatt, calculated as:

$$C_{Construction\_PL}=\sum_{i=1}^{r}\left(C_{PL\_i}\times PL_{Capacity\_i}\right) \quad (3)$$

Where C_{PL_i} is the construction cost of the i -th parking lot resource per kilowatt, $\mathrm{PL}_{Capacity\_i}$ represents the capacity of the i -th parking lot, and r is the number of requested parking lots.

$C_{Maintenance}$: Annual maintenance cost per kilowatt of installed capacity for DG and PL, calculated as:

$$C_{Maintenance}=\sum_{i=1}^{r}\left(C_{Maint}\times(DG_{Capacity\_i}+PL_{Capacity\_i})\right) \quad (4)$$

Where C_{Maint} are the maintenance costs for DG and PL per kilowatt per year, respectively.

P_{Loss} : Total active power losses in the network after installing parking lots and distributed generation resources, where the former is added as active power load to buses and the latter as a generator to buses, calculated according to Eq. (5):

$$P_{Loss}=\sum_{i=1}^{N_b} real(Z_{bi})\times {I_{bi}}^{2}{}_{DG\&PL} \quad (5)$$

Where Z_{bi} represents the impedance of the i -th branch, N_b is the number of branches obtained from the network specification table, and $I_{bi\ DG\&PL}$ is the branch current after installing parking lots and distributed generation resources, obtained from forward-backward load flow.

Q_{Loss} : Reactive power losses of buses after locating and sizing parking lots and distributed generation resources, calculated according to Eq. (6):

$$Q_{Loss}=\sum_{i=1}^{N_b} imag(Z_{bi})\times {I_{bi}}^{2}{}_{DG\&PL} \quad (6)$$

$$\begin{cases} V_{DI}=\dfrac{\sum_{i=1}^{n}(1-|V_i|)}{n} \\ \mathrm{P_{LRI}}=\dfrac{P_{Loss}}{P_{Lossbase}} \\ \mathrm{Q_{LRI}}=\dfrac{Q_{Loss}}{Q_{Lossbase}} \end{cases} \quad (7)$$

Where V_{DI} is the voltage deviation index, used to measure voltage deviation in the power network, n is the total number of network nodes, and V_i is the voltage of the i -th node after installing DG and PL.

$\mathrm{P_{LRI}}$: The ratio of increase or decrease in active power losses in the network after optimization compared to the initial state, P_{Loss} is the active power loss after optimization, and $P_{Lossbase}$ is the active power loss before optimization (or before installing DG and PL).

$\mathrm{Q_{LRI}}$: The ratio of increase or decrease in reactive power losses in the network after optimization compared to the initial state, Q_{Loss} is the reactive power loss after optimization, and $Q_{Lossbase}$ is the reactive power loss before optimization (or before installing DG and PL).

3- 2- Modeling Uncertainties

3- 2- 1- Modeling Wind Turbine Power Generation

Scenario generation for modeling uncertainty in wind turbine power generation should be performed by simulating wind speed uncertainty using the Weibull distribution function, defined as in Eq. (8) [14].

In this article, probability distribution functions such as the Weibull distribution for modeling wind speed and the Beta distribution for modeling solar radiation have been utilized. Additionally, the scenario generation and reduction method has been employed to manage uncertainties. However, the use of more advanced methods, such as Markov chains or Monte Carlo simulations, could enhance the accuracy of the modeling.

$$\begin{aligned} &V_{wi}=Wbl(\beta,\alpha)\ ,i=1,2,3,...,24 \\ &f(P_t^{WT})=\left(\frac{\beta}{\alpha^{\beta}}\right)(P_t^{WT})^{(\beta-1)}\,\mathrm{e}^{\left(-\left(\frac{P_t^{WT}}{\alpha}\right)^{\beta}\right)} \end{aligned} \quad (8)$$

Where $Wbl(\beta,\alpha)$ represents the Weibull distribution with parameters β,α and V_w is the wind speed obtained from meteorological data, β,α is the scale factor, and the

shape factor. i is the number of hours in a day. Since real data are used, β is set equal to the mean of V_w, and α is set to a positive integer (standard deviation of wind speed) to ensure that generated numbers in each scenario generation iteration fall within a realistic range. Here, $f(P_t^{WT})$ is the probability of power P_t^{WT} occurring at time t. The turbine power can then be calculated using the following Eq. (9):

$$P_W(v)=\begin{cases}0 & 0\le V_w\le v_{ci} \quad or \quad v_{ct}\le V_w\\ P_{\text{rated-w}}\times\left(\dfrac{v-v_{ci}}{v_r-v_{ci}}\right) & v_{ci}\le V_w\le v_r\\ P_{\text{rated-w}} & v_r\le V_w\le v_{ct}\end{cases} \quad (9)$$

Where $P_{\text{rated-w}}$ is the rated power of the turbine, v_{ci} is the minimum allowable speed for power generation, after which the turbine starts producing power, v_r is the rated speed of the wind turbine, and v_{ct} is the maximum allowable speed at which the turbine can produce power.

3- 2- 2- Modeling Solar Panel Power Generation

Scenario generation for modeling uncertainty in solar panel power generation should be performed by modeling the uncertainty in solar radiation intensity using the Beta probability distribution function, defined as in Eq. (10) [14]:

$$B(m_t,n_t)=\frac{\Gamma(m_t).\Gamma(n_t)}{\Gamma(m_t)+\Gamma(n_t)} \quad (10)$$

Where $B(m_t,n_t)$ is the Beta probability distribution function with parameters m_t and n_t, and to calculate them, the standard deviation of radiation per hour σ_t and the mean radiation per hour μ_t are needed. These are calculated using Eq. (11) and Eq. (12):

$$m_t=\mu_t.\left(\frac{\mu_t.(1-\mu_t)}{\sigma_t^2}-1\right) \quad (11)$$

$$n_t=(1-\mu_t).\left(\frac{\mu_t.(1-\mu_t)}{\sigma_t^2}-1\right) \quad (12)$$

Finally, the generated power is calculated using meteorological data based on radiation at different hours, according to Eq. (13):

$$f(P_t^{PV})=\frac{1}{B(m_t,n_t)}\left(\frac{P_t^{PV}}{P_{\max}^{PV}}\right)^{m_t-1}.\left(1-\frac{P_t^{PV}}{P_{\max}^{PV}}\right)^{n_t-1} \quad (13)$$

Where $f(P_t^{PV})$ is the probability of power P_t^{PV} occurring at the time t, and $P_{\max}^{PV}$ is the maximum power output of the panel.

3- 2- 3- Modeling Load Demand

A suitable probability distribution function is used for this purpose, employing the normal probability distribution function (PDF) as shown in Eq. (14) [15]. Using this equation, the probability of each scenario for the load can be calculated:

$$f(x)=\frac{1}{\sqrt{2\pi\sigma_{t,L}}}e^{\left(-\frac{(x-\mu_{t,L})^2}{2\sigma_{t,L}^2}\right)} \quad (14)$$

Where $\mu_{t,L}$ is the mean consumed load, and $\sigma_{t,L}$ is the standard deviation of the load.

3- 2- 4- Modeling Uncertainty in PHEV Behavior

The state of charge of a vehicle is SOC_{ar} upon arriving at the destination parking lot, P_{Ch} is the demand of each vehicle upon arrival, and Bat_i is the battery capacity of each vehicle. The article assumes two trips for each vehicle, with the premise that each vehicle returns to its initial parking lot (i.e., its residential location) after the second trip. Therefore, for different hours, two levels are considered for the charge level:

1. If the vehicle leaves the initial parking lot between 11 PM and 5 AM, the initial charge level is at its maximum, i.e., upon arriving at the next parking lot, the charge level is given by:

$$SOC_{ar}{}^{t}=SOC_{\max}-M_d\times E_m \quad (15)$$

$$P_{Ch}{}^{t}=SOC_{ar}{}^{t}\times Bat_i \quad (16)$$

This means that all vehicles must be fully charged when leaving their initial parking lot and participate in network optimization.

2. If the vehicle leaves the second parking lot between 10:30 AM and 4 PM, the vehicle's charge level is given by Eq. (17), as it may have discharged active power to the microgrid during this period:

$$SOC_{ar}{}^{t}=SOC_{trip}{}^{t}-M_d\times E_m \quad (17)$$

In the Eq. (17) SOC_{trip}, the battery capacity of each vehicle is considered to be between 30% and 50%. Additionally E_m, the energy consumption of each vehicle per mile traveled is calculated using Eq. (18) [16].

In this article, the modeling of electric vehicle behavior has primarily been based on travel patterns and battery charge levels. The impact of environmental factors, such as temperature, on battery performance has not been specifically examined. This could be considered a significant factor for more accurate modeling of battery behavior.

$$E_m = c.k_{PHEV} z \tag{18}$$

Where c and z are constant coefficients dependent on the type of PHEV, and k_{PHEV} represents the fraction of total input energy supplied by the battery. Next, the entry, exit, and travel times are expressed as:

$$\begin{cases} t_{trip1} = \mu_{trip1} + \sigma_{trip1}.N_1 \\ t_{dep1} = \mu_{dep1} + \sigma_{dep1}.N_2 \\ t_{ar1} = t_{dep1} + t_{trip1} \end{cases} \tag{19}$$

Where N_1 and N_2 are random variables, μ_{trip1} and σ_{dep1} are the mean and standard deviation of the first travel time based on historical data, μ_{dep1} and σ_{dep1} are the mean and standard deviation of the departure time, respectively, and t_{ar1} is the arrival time at the destination parking lot. For the second trip, only the statistical data differ, i.e., the mean and standard deviation values are different, but they are extracted using the same equations. These times are used to calculate the charging or discharging demand for the stations.

3- 3- Second Objective Function

In microgrid operation, the primary goal is to minimize the operator's operational costs while pursuing several essential objectives. These objectives include energy management and managing the charging/discharging demand of vehicles considering different prices and the profits of vehicle owners from V2G, increasing microgrid reliability, reducing losses, minimizing switching operations, reducing hours of connection to the upstream grid, and maintaining a balance between supply and demand. To achieve these objectives, microgrid charging and discharging scheduling is utilized. The objective function is multi-dimensional and includes various criteria that cannot be directly combined. To address this challenge, "fuzzy theory" is employed, which assigns maximum and minimum values to each objective using fuzzy membership functions [17]. The values obtained for each objective can be combined. This is expressed in Eq. (20).

Fuzzy theory was selected due to its ability to manage the inherent uncertainties of multiple objectives (such as the conflict between cost reduction and reliability enhancement). This method enables the conversion of qualitative objectives into quantitative ones and facilitates a balance between non-aligned criteria. Linear weighting and ε-constraint methods were also tested, but the results indicated that fuzzy theory, owing to its flexibility in defining membership functions, provides better convergence in the PSO-GA algorithm.

$$\min \sum_{i}^{n} F(X)_2 = \omega_i u_i(B_i) \tag{20}$$

Where $F(x)_2$ represents the fuzzy value obtained from combining objectives, B_i is the i -th objective, and the parameters u_i and ω_i are the fuzzy membership function and the weighting factor of the i -th objective, respectively.

$$B_i = \begin{cases} B_1 = P_{Loss} \\ B_2 = ENS \\ B_3 = T_{Ct} \\ B_4 = E_{Tr} \\ B_5 = N_{Sw} \\ B_6 = B_{parking} \end{cases} \tag{21}$$

Where P_{Loss} represents the active power losses at each hour in the network. To evaluate microgrid reliability, several indices are used to assess its independence and stability in supplying the consumed load [18]. A microgrid with a higher ability to supply its consumed load and reduce dependency on the main grid will perform better in terms of reliability. For this reason, the index ENS (Expected Energy Not Supplied), calculated using Eq. (22), T_{Ct} the index of hours the microgrid is connected to the upstream grid, calculated using Eq. (23), and E_{Tr} the index of energy received from the upstream grid, calculated using Eq. (25). Using the constraint in Eq. (28), all the above equations are calculated and incorporated into the objective function.

In the first objective function, constraints related to the maximum number of allowed distributed generation (DG) resources and parking lots (PLs) per bus, the prohibition of simultaneous placement of two parking lots or two DG resources on a single bus, the prohibition of simultaneous placement of a parking lot and a DG resource on a single bus, voltage deviation limits, and maximum branch current flow have been defined. In the second objective function, constraints including power balance at each time step, maximum power transfer between the upstream grid and the microgrid, and limits on the number of switching operations have been applied. These constraints prevent voltage instability, increased losses, and network overloading, thereby ensuring the dynamic stability of the system.

$$ENS = \frac{1}{T}\left(\sum_{i}^{T} ENS_i\right) \tag{22}$$

$$T_{Ct} = \frac{1}{T}\left(\sum_{i}^{T} C_i\right) \tag{23}$$

$$C=\begin{cases}0 & \text{if microgrid disconnected}\\ 1 & \text{if microgrid connected}\end{cases} \quad (24)$$

$$E_{Tr}=\frac{1}{T}\left(\sum_{i}^{T}E_{Tr_i}\right) \quad (25)$$

In the above equations, T_{Ct} represents the duration of the microgrid's connection to the main grid, C_i indicates whether the microgrid is disconnected or connected to the main grid at time i -th, E_{Tr} is the energy received by the microgrid from the main grid, and T is the microgrid's operational duration. Frequent switching between the microgrid and the main grid causes equipment wear and increases maintenance costs. By managing these switching operations and utilizing electric vehicles as flexible resources, the need for switching can be reduced. Vehicles, by discharging their batteries during peak consumption hours, supply the necessary energy and reduce dependency on the main grid.

$$N_{Sw}=\sum_{i}^{T}S_i \quad (26)$$

$$S=\begin{cases}0 & \text{if switch mode } i=\text{switch mode}(i-1)\\ 1 & \text{if switch mode } i\neq\text{switch mode}(i-1)\end{cases} \quad (27)$$

Where N_{Sw} is the number of switching operations during the operational period, S_i indicates whether the switch is open or closed, $\text{switch mode } i$ indicates the open or closed status of the switch at the time i, and $\text{switch mode}(i-1)$ indicates the open or closed status of the switch at time i.

$$\sum_{t}^{24}P_G{}^{t}+\sum_{t=1}^{24}\sum_{i=1}^{N_{phev}}P_{Disch,i}{}^{t}+\sum_{t=1}^{24}P_{DG}{}^{t}=\sum_{t=1}^{24}P_D{}^{t}+\sum_{t=1}^{24}\sum_{i=1}^{N_{phev}}P_{Ch,i}{}^{t}+\sum_{t=1}^{24}P_{Loss}{}^{t} \quad (28)$$

The above equation represents the power balance constraint in the microgrid at time t. P_G is the maximum power transferred from the main grid to the microgrid, which is zero for all buses except the input bus of the microgrid. $P_{disch,i}$ is the discharge power of the i -th vehicle at time t, determined by the discharge scheduling management based on network needs. P_{DG} is the active power generated by distributed generation resources, and P_D is the microgrid's consumed power at time t, which was previously modeled in the uncertainty section for load consumption and generation resources, and their outputs are used here. $P_{Ch,i}$ is the charging demand of the i -th vehicle upon entering the parking lot at time t. Like discharging, this can be scheduled for charging instead. Finally, P_{Loss} is the power loss at time t. However, the parameter $B_{parking}$ in Eq. (29) represents the profit of the parking lot from charging and discharging:

$$B_{parking}=C(t)\times\sum_{t=1}^{24}\sum_{i=1}^{N_{phev}}P_{Ch,i}{}^{t}-C(t)\times\sum_{t=1}^{24}\sum_{i=1}^{N_{phev}}P_{Disch,i}{}^{t}-CD_{Bat}\times\sum_{t=1}^{24}\sum_{i=1}^{N_{phev}}P_{Disch,i}{}^{t} \quad (29)$$

$$C(t)=\begin{cases}0.4 & \text{if } t\in(\text{Not peak demand time})\\ 0.6 & \text{if } t\in(\text{peak demand time})\end{cases}$$

CD_{Bat} refers to battery degradation, $C(t)$ is the price of energy purchased by the parking lot from the microgrid, and the energy purchased from the upstream grid, varying with time. Based on the above objective functions and formulation, the proposed algorithm can be illustrated in the flowcharts below. For the first objective function, the flowchart in Fig. 1 is used, and for the second objective function, the flowchart in Fig. 2 is used. For simulations, the hybrid PSO-GA metaheuristic algorithm from reference [19] is utilized.

4- Numerical Simulation

In this section, the study is conducted on a 69-bus network, and all simulations are performed in the MATLAB software environment, with the simulation outputs discussed.

4- 1- Information on the Studied Microgrid

Various structures can be considered for microgrids. In this study, the standard IEEE 69-bus microgrid is used, as shown in Fig. 3. The technical specifications and network information are presented in [20].

The costs mentioned in the first objective function for determining the optimal location and capacity of PL and DG are specified, with a cost criterion based on several references provided in Table 1.

4- 2- Network Analysis in Base Load Condition

The specifications of active and reactive power losses and voltage drop before locating PL and DG in the microgrid are provided in Table 2, and the voltage profile is shown in Fig. 4.

4- 3- Microgrid Specifications with Simultaneous Locating and Sizing of PL and DG

In this section, PLs are considered as loads, meaning V2G capability is not considered at this stage, yielding favorable results. It is noted that for 500 plug-in hybrid electric vehicles, 5 parking lots are considered. To ensure load response capability and islanded operation of the microgrid, 8 distributed generation resources are located. The simulation results are provided in Table 3, and the voltage profile is shown in Fig. 5.

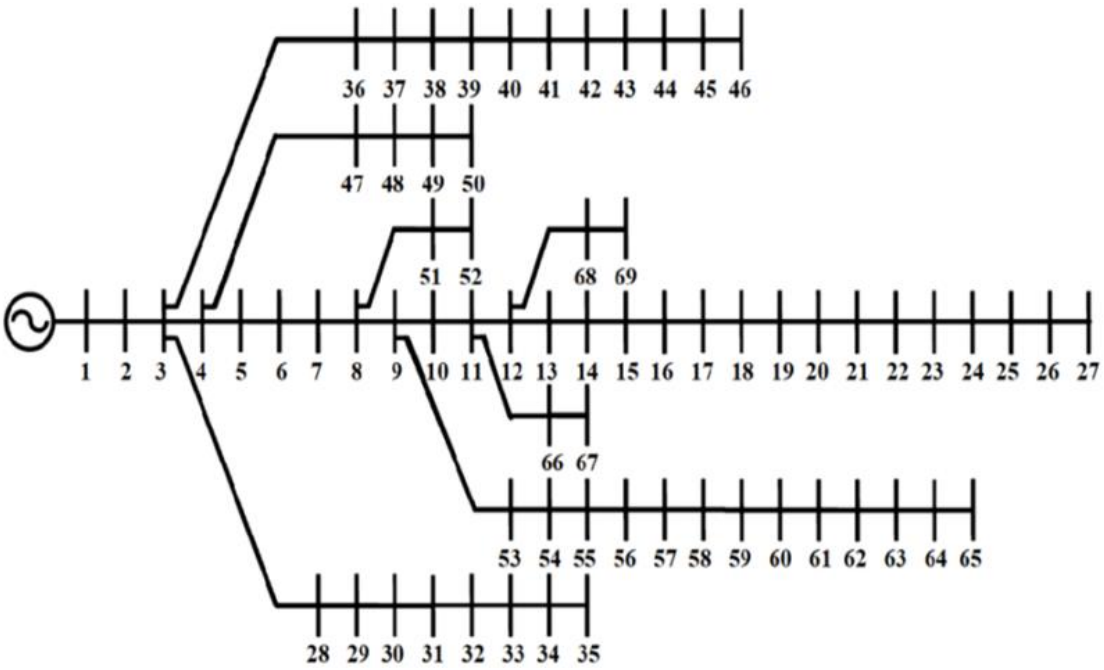

Fig. 3. Structure of the 69-bus microgrid.

Table 1. Cost values in the first objective function.

Cost	Parameter	Value
Cost of active power losses	C_{Ploss}	0.4 dollars per kilowatt-hour
Cost of reactive power losses	C_{Qloss}	0.1 dollar per kiloVAr-hour
DG construction cost	$C_{Construction\_DG}$	3000 dollars per kilowatt
PL construction cost	$C_{Construction\_PL}$	2000 dollars per kilowatt
DG and PL maintenance cost	$C_{Maintenance}$	50 dollars per kilowatt per year
Cost of energy received from the main grid and the Cost of charging and discharging during off-peak hours	$C(t)$	0.4 dollars per kilowatt
Cost of energy received from the main grid and Cost of charging and discharging during peak hours	$C(t)_{peak}$	0.6 dollars per kilowatt
Battery degradation cost	CD_{Bat}	0.02 dollars per kilowatt

Table 2. Bus specifications before locating PL and DG.

Active power losses (KW)	221.7827
Reactive power losses (KVAr)	100.7909
Minimum voltage (p.u.)	9.0988
Bus number with the lowest voltage	65

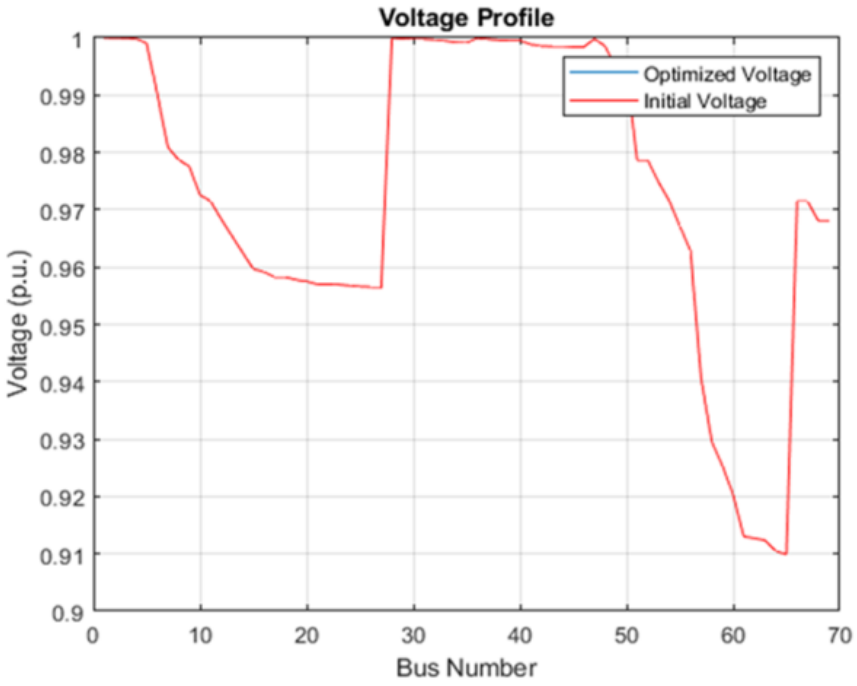

Fig. 4. Voltage profile of the entire microgrid before locating PL and DG.

Table 3.Microgrid specifications after simultaneous locating and sizing of PL and DG.

Location and capacity of DGs	DG_1	In busbar 8 with a capacity of 347.42 kilowatts
	DG_2	In busbar 12 with a capacity of 355.16 kilowatts
	DG_3	In busbar 22 with a capacity of 1367.10 kilowatts
	DG_4	In busbar 26 with a capacity of 1151.80 kilowatts
	DG_5	In busbar 43 with a capacity of 969.87 kilowatts
	DG_6	In busbar 49 with a capacity of 1016.20 kilowatts
	DG_7	In busbar 61 with a capacity of 1649.80 kilowatts
	DG_8	In busbar 64 with a capacity of 153.66 kilowatts
Location and capacity of PLs	PL_1	In busbar 21 with a capacity of 938.98 kilowatts
	PL_2	In busbar 25 with a capacity of 1.2381 kilowatts
	PL_3	In busbar 36 with a capacity of 1200.70 kilowatts
	PL_4	In busbar 44 with a capacity of 814.18 kilowatts
	PL_5	In busbar 47 with a capacity of 806.02 kilowatts
Minimum voltage (per unit)		0.98355
Bus number with the lowest voltage		65
Active power losses (KW)		70.188
Reactive power losses (KVAr)		32.3542
Loss reduction		68.5301 percent
Profit from loss reduction		591,271 dollars per year
Cost (construction, maintenance, and losses)		31,831,950 dollars

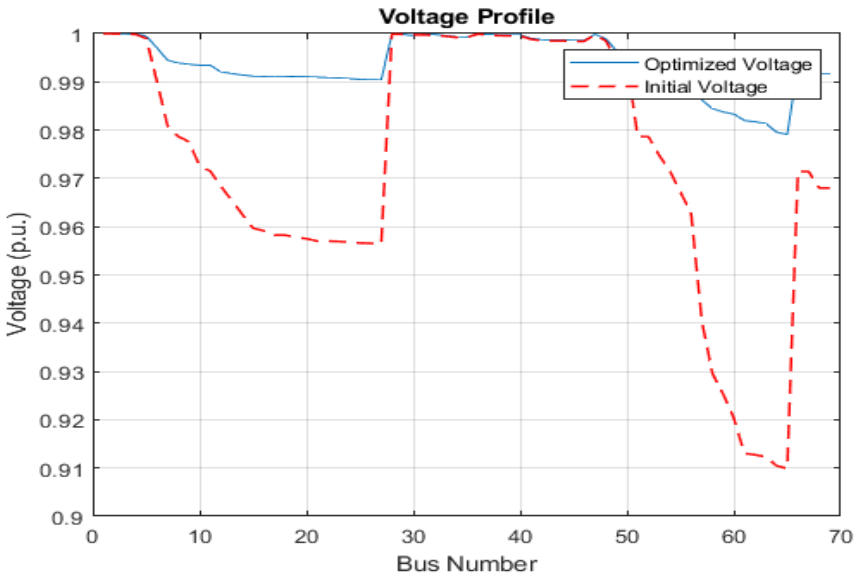

Fig. 5. Voltage profile of the microgrid after simultaneous locating and sizing of PL and DG.

This article addresses the simultaneous improvement of active and reactive power losses and the reduction of construction and maintenance costs of microgrid infrastructure. By simultaneously locating and sizing 8 DG units with a total capacity of 7 MW and 5 MW of PL load, active and reactive losses were reduced by 68.53% and 67.89%, respectively. Without location and capacity constraints, these values could exceed 70%. The minimum voltage reached 0.98355 p.u., and the voltage deviation improved. Additionally, the annual profit from loss reduction was estimated at $591,271. The DG specifications include wind turbines with 6 units of 275 kW (1.65 MW) at bus 61, 5 units of 275 kW (1.375 MW) at bus 21, and 5 units of 200 kW (1 MW) at bus 49. Additionally, a 969.87 kW microturbine with 97% efficiency at bus 43 and solar systems with various capacities, including 0.34742 MW at bus 8, are considered.

4- 4- Results of Uncertainty Modeling

For scenario reduction, according to reference [21], the distance between generated scenarios is first calculated. Then, for each scenario, the scenario with the closest distance to it is determined. In the final stage, scenarios with the smallest distance from each other are selected. Then, by multiplying the occurrence probability of each scenario by its distance from the closest scenario, it is determined which scenario has the least impact, and that scenario is eliminated. Uncertainty modeling uses meteorological data for Tehran, the capital of Iran, on July 11, 2024, for the summer season, obtained from the reference meteorological website [22].

4- 4- 1- Modeling Wind Turbine Output Power

In this article, the output power of four wind turbines for 24 hours is modeled using the scenario generation and reduction method, where from 200 generated scenarios, 24 scenarios with the highest similarity are selected, and ultimately, one final scenario is chosen. Fig. 6(a) shows the generated and selected scenarios for the output power of a 1650 kW wind turbine and their associated probabilities. Fig. 6(b) shows a graph of the 24 selected scenarios from among 200 scenarios.

The same process is performed for wind turbines with capacities of 1.1 MW, 1.375 MW, and 1 MW.

4- 4- 2- Modeling Solar Panel Output Power

The output power of the panels for 24 hours is modeled in 200 different scenarios, and 24 scenarios with the highest similarity to each other are selected, with one final scenario chosen. For buses 8 and 12, the same pattern is used. The third panel is modeled similarly. In Fig. 7(a), the generated and remaining scenarios for the output power of solar panels with a capacity of 350 kW, along with the probability of each scenario, are shown. Fig. 7(b) shows a graph of the 24 selected scenarios from among 200 scenarios.

4- 4- 3- Modeling Load Demand Uncertainty

For this modeling, load consumption data from the distribution network reference [23] are used. Fig. 8 shows the stages of scenario generation and selection for modeling load uncertainty along with the data used.

4- 4- 4- Modeling PHEV Behavior

This study addresses the optimal management of charging and discharging of 500 plug-in hybrid electric vehicles (PHEVs) in microgrid parking lots. Using statistical data, the behavior of charging, discharging, distance traveled, entry and exit times, and battery charge levels is modeled. Vehicles, during two daily trips with

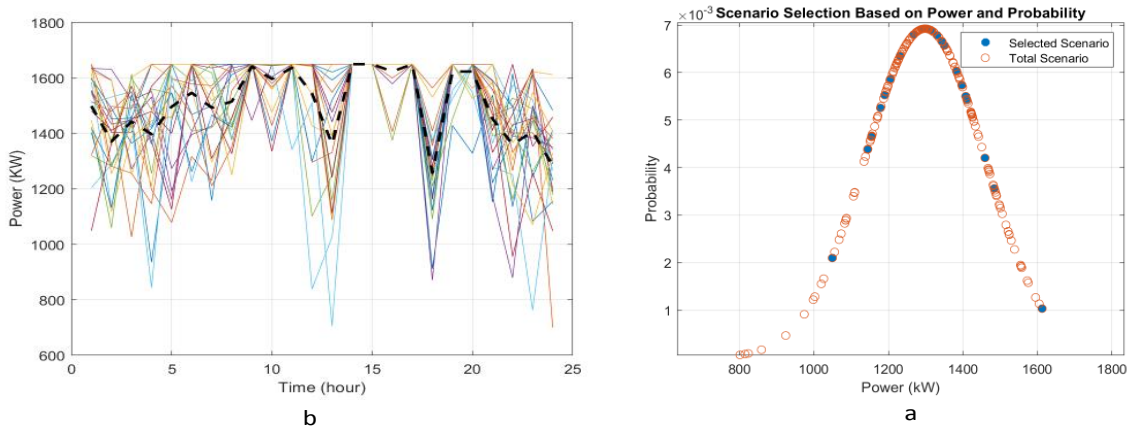

Fig. 6. Generated and remaining scenarios for wind turbine output power along with the probability of each scenario.

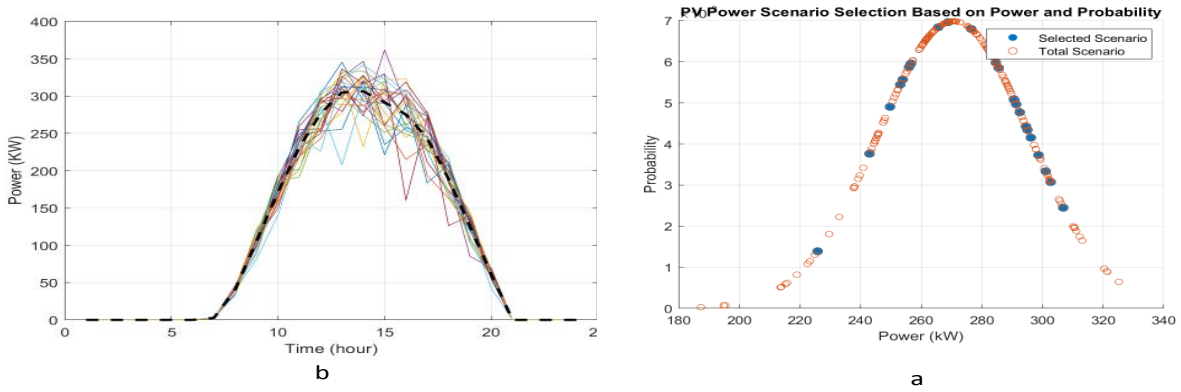

Fig. 7. Generated and remaining scenarios for solar panel output power, along with the probability of each scenario.

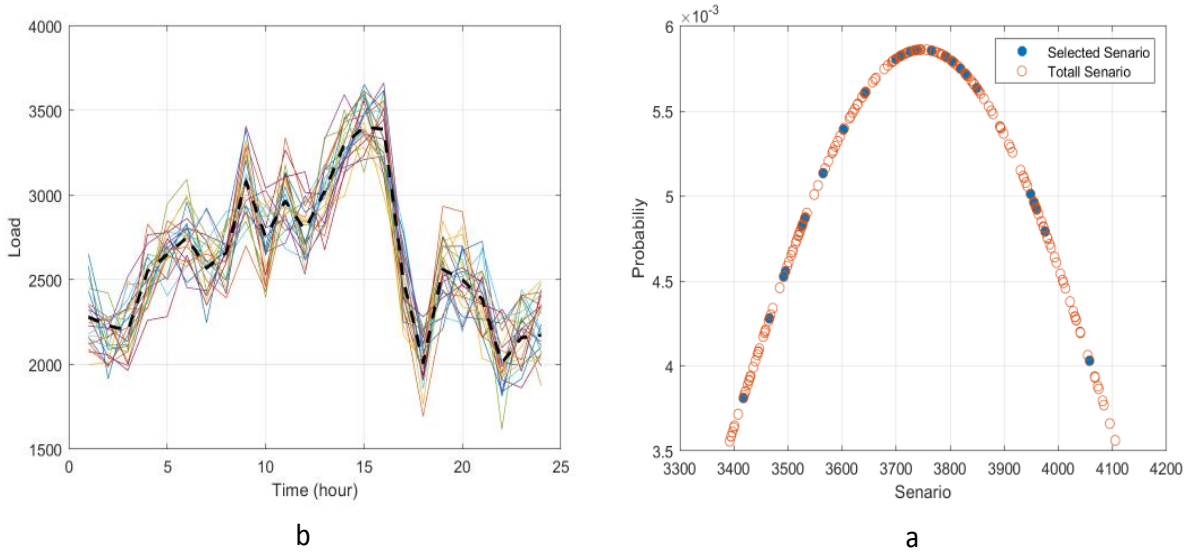

Fig. 8. (a) Generated and remaining scenarios for network load demand along with the probability of each scenario. (b) Graphs of 24 selected scenarios from 200 scenarios generated for modeling network load demand, along with the data used for scenario generation.

Table 4. Specifications required for simulating PHEV uncertainty.

Time (hours) and distance	Mean	Standard deviation
Exit from Parking 1	6.30	1.5
Exit from Parking 2	16	1.5
First travel	1.5	1
Second travel	1.5	1
Distance of travel 1 (miles)	30	5
Distance of travel 2 (miles)	35	5

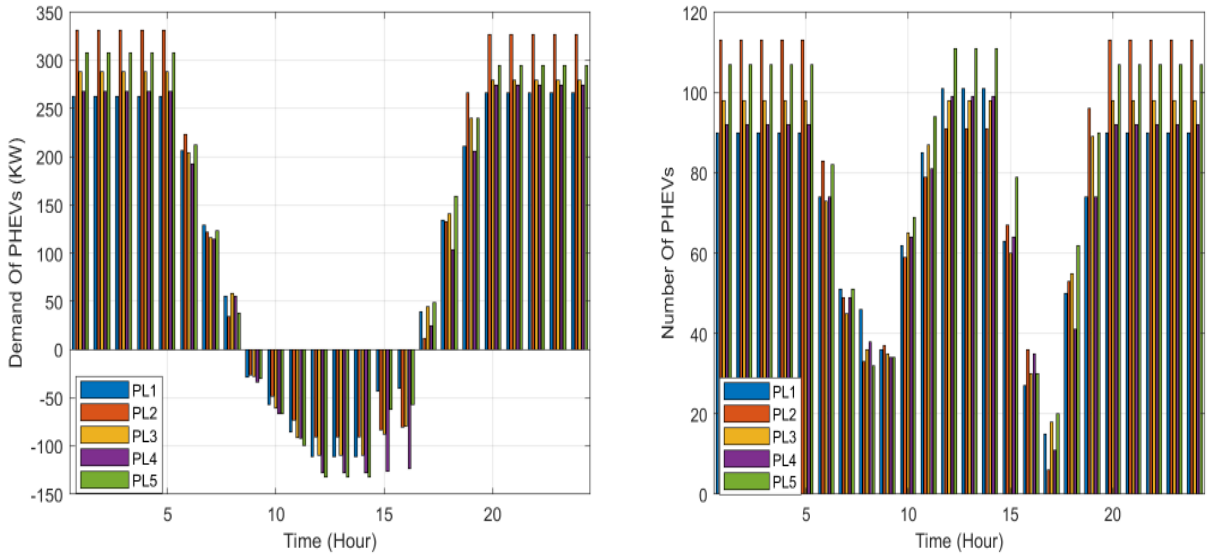

Fig. 9. (a) Number of vehicles present in each parking lot per hour. (b) Amount of power requested for charging per hour. Note that the negative part of the graph does not necessarily indicate discharging; it represents the energy available for discharge to the network, as charging/discharging scheduling is not performed in this section.

specified mean and standard deviation, are transferred to the workplace and residential parking lots. The mean and standard deviation specifications are provided in Table 4. According to the equations, various values for exit times from parking lots, travel duration, arrival times at parking lots, distance traveled, energy consumed, charging demand, and remaining charge levels are generated. Battery capacity and energy consumption for PHEVs are obtained from reference [24] and shown in Table 5.

Based on the above explanations, with modeling as shown in Fig. 9, part (a) provides the results for entry and exit hours from parking lots and the number of vehicles present in the parking lots, and part (b) of Fig. 9 provides the amount of energy required for charging vehicles.

4- 5- Optimal Operation of the Microgrid in the Presence of PHEV Parking Lots and Various Uncertainties

Based on the data obtained from uncertainty modeling and the combined objectives of the second objective function, optimization of costs, increased energy efficiency, improved stability, and reduced losses are pursued to achieve optimal performance for the microgrid. It is assumed that the output power of distributed generation resources is directly injected into the main bus, and the upstream grid power (800 to 2000 kW) is calculated with simulated random values for 24 hours. The data obtained are shown in Table 6. In this article, the focus has primarily been on energy management and loss reduction; however, the specific impact of frequency and voltage fluctuations resulting from the charging and

Table 6. Data required for the second objective function.

time	Energy transferable from the upstream grid (kilowatt)	The power generation of DGs (kilowatt)	Load demand (kilowatt)
1	1656.9	6080.008	2449.950
2	1839.6	5572.675	2421.733
3	1854.7	5696.581	2086.873
4	1262	5442.697	2652.594
5	1165.9	5613.243	2618.607
6	1519.3	5691.192	2768.276
7	1769.1	4485.394	2708.813
8	1700.1	6102.088	2505.573
9	1589.7	6141.428	3239.389
10	1907.1	6435.343	2673.206
11	1399.7	6605.059	2791.098
12	1900	6775.029	2826.785
13	1144.7	6593.504	2817.578
14	1196	6936.164	3159.949
15	1590.1	6870.879	3213.455
16	1469.4	6799.348	3181.305
17	1432.9	6699.209	2433.664
18	11915	5639.908	1907.237
19	1254.7	6417.531	2703.049
20	1072	6196.803	2616.863
21	914.77	5140.086	2158.126
22	877.13	5384.098	2274.266
23	931.38	5603.853	2244.1591
24	1167	5347.823	2481.244

Table 7. Results obtained for microgrid operation without charging and discharging scheduling.

Energy Not Supplied (ENS)	0
Energy received from the upstream grid by the microgrid (kilowatt-hour)	764.37
Duration of connection to the upstream grid (hours)	11
Number of switching operations to the upstream grid	9
Losses (kilowatt)	4483.1
Amount of power transferred from the parking lots (kilowatt)	-5174.6
Amount of power received by the parking lots (kilowatt)	16721

discharging of electric vehicles has not been addressed. This topic could be considered an important aspect for future research.

4- 5- 1- Microgrid Operation Without Charging and Discharging Scheduling

Microgrid operation without charging/discharging scheduling for 500 plug-in hybrid electric vehicles, using data from the first objective function and uncertainty modeling, and adding additional load to all buses, yields results in Table 7.

4- 5- 2- Microgrid Operation With Charging and Discharging Scheduling

In this scenario, the optimal operation of the microgrid with charging/discharging scheduling for 500 plug-in hybrid electric vehicles is addressed using fuzzy theory with the PSO-GA algorithm, yielding results in Table 8.

The proposed model, by simultaneously optimizing the locating and operation of distributed generation (DG) resources and electric vehicle parking lots (PLs), aims to maximize the utilization of the microgrid's internal resources.

Table 8. Results obtained for microgrid operation with charging/discharging scheduling using the proposed algorithm.

Energy Not Supplied (ENS)	0
Energy received from the upstream grid by the microgrid (kilowatt-hours)	0
Duration of connection to the upstream grid (hours)	0
Number of switching operations to the upstream grid	0
Losses (kilowatt)	3604.5
Amount of power transferred from parking lots(kilowatt)	-10313
Amount of power received by parking lots(kilowatt)	25493

In the second objective function, intelligent management of electric vehicle charging and discharging, based on real-time electricity prices and network conditions, ensures increased stability and reduced need for power exchange with the upstream grid. Additionally, constraints related to the minimum hours of microgrid independence in operation have enabled the network to operate in islanded mode for 24 hours in the optimal scenario, demonstrating enhanced resilience and reduced dependence on the main grid.

Uncertainties related to load forecasting, renewable resource generation (wind and solar), and electric vehicle behavior have been incorporated into the operation modeling. The scenario generation and reduction method has reduced the number of scenarios analyzed without compromising the accuracy of the analysis, thereby enhancing decision-making efficiency. On the other hand, by employing fuzzy theory in the second objective function, the model can balance objectives such as maximizing profit, reducing losses, and increasing reliability. These mechanisms have enabled the model to maintain stable and optimal performance under fluctuations in renewable resources and unforeseen changes in load behavior.

In Fig. 10, the first bar (blue) represents the parking lot at bus 21, the second bar (red) represents the parking lot at bus 25, the third bar (yellow) represents the parking lot at bus 36, the fourth bar (purple) represents the parking lot at bus 44, and the fifth bar (green) represents the parking lot at bus 47. This scenario, with simulation results shown in Table 7, indicates that the microgrid operated entirely in islanded mode for 24 hours, fully meeting all load demands. This demonstrates complete independence from the upstream grid and increased resilience in energy supply. Additionally, active power losses in this scenario were significantly reduced, and energy efficiency was optimized. In this scenario, electric vehicles with V2G capability acted as rotating energy storage resources, reducing active power losses by 19.6% compared to the second scenario (operation without scheduling). This improvement played a significant role in increasing system stability and meeting load demands. As observed in Fig 12, part (c), power losses, even at their peak, were below 200 kW, as in the base load condition without additional demand and PHEV loads, power losses were 221 kW per hour, and with the addition of these loads, they decreased to a maximum of 194.5 kW. This indicates improved network performance in terms of loss reduction.

5- Conclusion and Recommendations

In this article, aiming to reduce operational costs and improve microgrid performance, a comprehensive approach based on multi-objective optimization and uncertainty modeling is presented. The results show that the optimal locating and sizing of electric vehicle parking lots and distributed generation resources, in addition to reducing power losses (68.35% in active power and 67.89% in reactive power), contribute to improved voltage profiles and reduced construction and maintenance costs. This improvement is primarily due to the optimal locating of distributed generation (DG) resources in the first stage, where parking lots are considered as loads. In the second stage, the participation of electric vehicles through vehicle-to-grid (V2G) technology contributed to reducing peak loads and helped achieve a 19.6% reduction in losses. This is because, in this stage, additional loads and uncertainties in the power generation of renewable resources are taken into account, and electric vehicles undertake two trips.

Furthermore, the use of electric vehicles as energy storage units and optimal control of their charging/discharging have led to increased efficiency, reduced switching operations, and improved network stability. In the second stage, optimal microgrid operation with the mentioned objectives, using the hybrid PSO-GA algorithm, yielded precise results, demonstrating that adding load demand at all hours and electric vehicle loads to buses can reduce losses by up to 19.6%. This research indicates that microgrids equipped with electric vehicle technology and distributed generation resources can enhance the efficiency and flexibility of power systems, significantly reduce operational costs, improve network performance, and mitigate environmental impacts, serving as a reference for the development of sustainable energy systems.

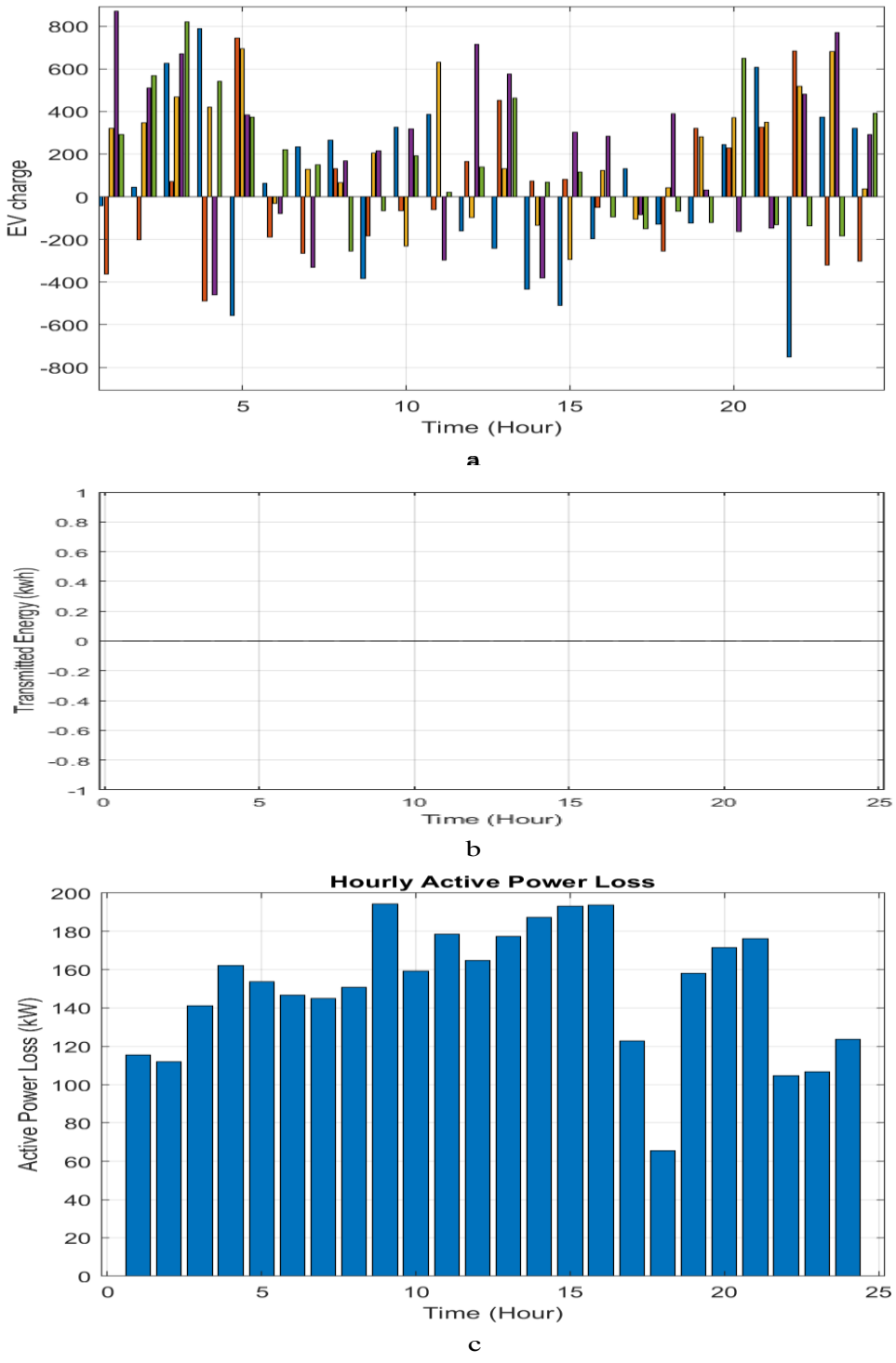

Fig. 10. (a) Charging and discharging scheduling using fuzzy theory with the PSO-GA algorithm. (b) Amount of energy received by the microgrid from the upstream grid and hours of connection/disconnection to the grid. (c) Active power losses of the microgrid over 24 hours.

References

[1] C. Yang, Y. Zhao, X. Li, and X. Zhou, "Innovative Strategies for Grid Resilience: Electric Vehicles, Load Response, and Renewable Energy Synergy in the Smart Grid Era," Renewable Energy, p. 121890, 2024.

[2] S. R. Salkuti, "Optimal operation of microgrid considering renewable energy sources, electric vehicles and demand response," in E3S web of conferences, 2019, vol. 87, p. 01007: EDP Sciences.

[3] M. Nour, J. P. Chaves-Ávila, G. Magdy, and Á. Sánchez-Miralles, "Review of positive and negative impacts of electric vehicles charging on electric power systems," Energies, vol. 13, no. 18, p. 4675, 2020.

[4] S. Shojaei, J. Beiza, T. Abedinzadeh, and H. Alipour, "Optimal energy and reserve management of a smart microgrid incorporating parking lot of electric vehicles/ renewable sources/responsive-loads considering uncertain parameters," Journal of Energy Storage, vol. 55, p. 105540, 2022.

[5] S. Ray, K. Kasturi, S. Patnaik, and M. R. Nayak, "Review of electric vehicles integration impacts in distribution networks: Placement, charging/discharging strategies, objectives and optimisation models," Journal of Energy Storage, vol. 72, p. 108672, 2023.

[6] A. K. Karmaker, M. A. Hossain, H. R. Pota, A. Onen, and J. Jung, "Energy management system for hybrid renewable energy-based electric vehicle charging station," IEEE Access, vol. 11, pp. 27793-27805, 2023.

[7] M. H. Amini, M. P. Moghaddam, and O. Karabasoglu, "Simultaneous allocation of electric vehicles' parking lots and distributed renewable resources in smart power distribution networks," Sustainable cities and society, vol. 28, pp. 332-342, 2017.

[8] L. Chen, C. Xu, H. Song, and K. Jermsittiparsert, "Optimal sizing and siting of EVCS in the distribution system using metaheuristics: A case study," Energy Reports, vol. 7, pp. 208-217, 2021.

[9] A. Mohsenzadeh, S. Pazouki, S. Ardalan, and M.-R. Haghifam, "Optimal placing and sizing of parking lots including different levels of charging stations in electric distribution networks," International Journal of Ambient Energy, vol. 39, no. 7, pp. 743-750, 2018.

[10] M. Z. Zeb et al., "Optimal placement of electric vehicle charging stations in the active distribution network," IEEE Access, vol. 8, pp. 68124-68134, 2020.

[11] M. Ahmadi et al., "Optimal allocation of EVs parking lots and DG in micro grid using two-stage GA-PSO," The Journal of Engineering, vol. 2023, no. 2, p. e12237, 2023.

[12] P. Aliasghari, B. Mohammadi-Ivatloo, M. Alipour, M. Abapour, and K. Zare, "Optimal scheduling of plug-in electric vehicles and renewable micro-grid in energy and reserve markets considering demand response program," Journal of Cleaner Production, vol. 186, pp. 293-303, 2018.

[13] S. Gupta, A. Maulik, D. Das, and A. Singh, "Coordinated stochastic optimal energy management of grid-connected microgrids considering demand response, plug-in hybrid electric vehicles, and smart transformers," Renewable and Sustainable Energy Reviews, vol. 155, p. 111861, 2022.

[14] Y. Wang, X. Ai, Z. Tan, L. Yan, and S. Liu, "Interactive dispatch modes and bidding strategy of multiple virtual power plants based on demand response and game theory," IEEE Transactions on Smart Grid, vol. 7, no. 1, pp. 510-519, 2015.

[15] D. Wang, J. Qiu, L. Reedman, K. Meng, and L. L. Lai, "Two-stage energy management for networked microgrids with high renewable penetration," Applied Energy, vol. 226, pp. 39-48, 2018.

[16] M. H. Amini, A. Kargarian, and O. Karabasoglu, "ARIMA-based decoupled time series forecasting of electric vehicle charging demand for stochastic power system operation," Electric Power Systems Research, vol. 140, pp. 378-390, 2016.

[17] Z. F. Allami, H. M. Abid, B. A. Mohammed, A. A. Ali, Z. L. Naser, and M. M. Abdulhasan, "A Renewable Microgrid with Hydrogen for Residential Use: Fuzzy Logic for Multi-Objectives," International Journal of Renewable Energy Research (IJRER), vol. 14, no. 1, pp. 31-37, 2024.

[18] A. Kumar, A. Verma, and R. Talwar, "Optimal techno-economic sizing of a multi-generation microgrid system with reduced dependency on grid for critical health-care, educational and industrial facilities," Energy, vol. 208, p. 118248, 2020.

[19] H. Garg, "A hybrid PSO-GA algorithm for constrained optimization problems," Applied Mathematics and Computation, vol. 274, pp. 292-305, 2016.

[20] C. Venkatesan, R. Kannadasan, M. H. Alsharif, M.-K. Kim, and J. Nebhen, "A novel multiobjective hybrid technique for siting and sizing of distributed generation and capacitor banks in radial distribution systems," Sustainability, vol. 13, no. 6, p. 3308, 2021.

[21] Y. Xu, Z. Y. Dong, R. Zhang, and D. J. Hill, "Multi-timescale coordinated voltage/var control of high renewable-penetrated distribution systems," IEEE Transactions on Power Systems, vol. 32, no. 6, pp. 4398-4408, 2017.

[22] [TBD: Reference for meteorological data].

[23] W. S. Tan, M. Y. Hassan, H. A. Rahman, M. P. Abdullah, and F. Hussin, "Multi-distributed generation planning using hybrid particle swarm optimisation-gravitational search algorithm including voltage rise issue," IET Generation, Transmission & Distribution, vol. 7, no. 9, pp. 929-942, 2013.

[24] O. Hafez and K. Bhattacharya, "Queuing analysis based PEV load modeling considering battery charging behavior and their impact on distribution system operation," IEEE Transactions on Smart Grid, vol. 9, no. 1, pp. 261-273, 2016.

HOW TO CITE THIS ARTICLE
M. Alizadeh, R. Eslami, A. R. Salmani, Microgrid Operation Optimization Using Optimal Locating and Sizing of PHEV Parking Lots Considering Various Uncertainties , AUT J. Elec. Eng., 57(3) (2025) 569-588.

DOI: 10.22060/eej.2025.24194.5660